Tracking the distribution of persistent and mobile wastewater-derived substances in the southern and central North Sea using anthropogenic gadolinium from MRI contrast agents as a far-field tracer

Dennis Kraemer [a,*], Katja Schmidt [a], Franziska Klimpel [b], Uwe Rauch [a], David M. Ernst [b], Sophie A.L. Paul [b,c], Matthias Haeckel [c], Andrea Koschinsky [b], Michael Bau [b]

[a] *Federal Institute for Geosciences and Natural Resources (BGR), Stilleweg 2, 30655 Hannover, Germany*
[b] *School of Science, Constructor University Bremen, Campus Ring 1, 28759 Bremen, Germany*
[c] *GEOMAR Helmholtz Centre for Ocean Research Kiel, 24148 Kiel, Germany*

ARTICLE INFO

ABSTRACT

The use of the rare earth element gadolinium (Gd) in contrast agents for magnetic resonance imaging has led to a significant (micro-)contamination of riverine and coastal environments in many parts of the world. This study comprises a detailed investigation on the rare earth elements and yttrium inventory of the North Sea and also reports data for the major tributaries Thames, Rhine, Ems, Weser and Elbe. We show that large parts of the southern North Sea, including the Wadden Sea UNESCO Natural World Heritage site, are (micro)contaminated with Gd from Gd-based contrast agents (GBCA). Their dispersion reveals their estuarine input and allows to effectively track water masses and currents. The chemical persistence and conservative behavior of GBCA, coupled with the low detection limits of state-of-the-art analytical methods, makes the anthropogenic Gd a sensitive screening proxy for monitoring similarly stable, but potentially hazardous, persistent chemical/pharmaceutical substances in natural waters.

1. Introduction

In the last decades, many trace elements gained societal and economic importance due to growing demand for high-technology products and processes, for example in the medical, electromobility and renewable energy sectors. Their increasing application in enabling technologies results in a quickly growing and largely unconstrained pollution of the environment. Knowledge of the anthropogenic input fluxes, the behavior in the environment and the (eco)toxicological effects are for many of these elements still scarce. Since the late 1980s, the rare earth element gadolinium (Gd) is routinely used in medical diagnostics as a contrast agent for magnetic resonance imaging (MRI) due to its paramagnetic property. The free Gd^{3+} ion, however, is highly toxic for living organisms even at low concentrations (Idée et al., 2008; Vassallo et al., 2011). It is thus usually administered as a water-soluble linear or macrocyclic complex, with recent prevalence for the latter because of an EU-wide ban of linear complexes due to the potential release of Gd from the ligand and incorporation into human bones (Darrah et al., 2009; Turyanskaya et al., 2020) and/or deposition in the brain (Kanda et al.,

2016a, 2016b). According to the European Medicines Agency (2017), the currently most widely used forms of Gd-based contrast agents (GBCAs) are the linear-complexed gadopentetate dimeglumine (Gd-DTPA, Magnevist©; banned in the EU) and the macrocyclic GBCAs gadoteridol/gadobutrol (Gd-HP/BT-DO3A; ProHance©, Gadovist©) and gadoterate meglumine (Gd-DOTA; Dotarem©). Due to the stable chemical complexation, these GBCAs usually leave the body via renal excretion within the first 24–30 h after injection and enter the sewage system. As a result of their unreactive nature, only about 10 % of the GBCAs, mostly the less stable linear complexes, are effectively removed during conventional waste water treatment (Telgmann et al., 2012b), unless advanced techniques like ozonation are employed (Lawrence et al., 2010). Thus, the majority of GBCAs are introduced via the effluents into surface waters such as rivers, lakes and coastal seawater (e.g., Kulaksız and Bau, 2013).

Since its first detection in rivers in Central Europe and North America almost thirty years ago (Bau and Dulski, 1996), the presence of anthropogenic Gd and Gd-based MRI contrast agents have been reported in countries with highly developed health care systems for almost every

---

* Corresponding author.
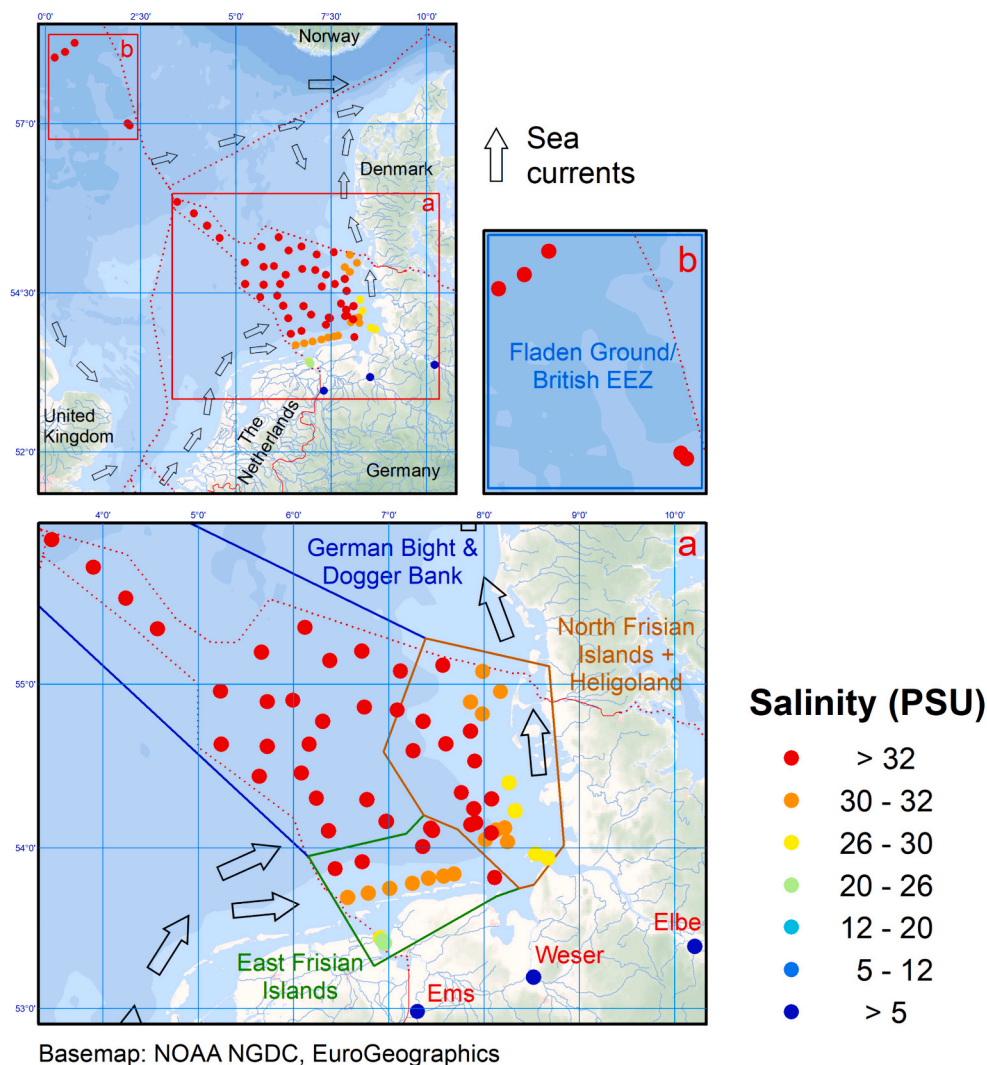 *E-mail address:* dennis.kraemer@bgr.de (D. Kraemer).

Fig. 1. Overview of the reported sampling stations, salinities and the division into the subgroups used for presentation and discussion of the data. Note that water from the Thames and the Rhine rivers enters the study area from the English Channel/the Southern Bight. Major water currents are indicated by the black arrows according to OSPAR Commission (2000) and Turrell (1992).

large river and lake (e.g., Bau et al., 2006; Birka et al., 2016b, 2013; Horstmann et al., 2021; Kreitsmann and Bau, 2023; Kulaksız and Bau, 2007; Kulaksız and Bau, 2013; Lerat-Hardy et al., 2019; Louis et al., 2023; Macke et al., 2021; Merschel et al., 2015; Raju et al., 2010; Zhang et al., 2024) as well as in groundwater (due to recharge with contaminated river and/or lake water via bank filtration; e.g., Brünjes et al., 2016; Möller et al., 2011). Although the anthropogenic Gd microcontamination is not considered toxic at the currently observed low concentrations, the understanding of the long-term effects of prolonged exposure to GBCAs and the release of Gd^{3+} from the ligands are still limited (Birka et al., 2016a; Telgmann et al., 2012a). Oral uptake of GBCAs with beverages or food may be a concern, as recent research suggests that GBCAs, especially of linear complexes, may be partially decomposed in the body upon oral uptake (Souza et al., 2021). Indeed, Gd from GBCAs may enter the food chain via tap water and beverages (Bau and Dulski, 1996; Birka et al., 2016b; Krohn et al., 2024; Kulaksız and Bau, 2011; Lindner et al., 2015; Möller et al., 2000; Schmidt et al., 2019; Tepe et al., 2014; Wysocka et al., 2023). Current research suggests that the majority of GBCAs in natural systems is *not* bioavailable, as indicated by several studies on bivalves (Alemu et al., 2024; Barrat et al., 2022; Hanana et al., 2017; Henriques et al., 2019; Merschel et al., 2015; Perrat et al., 2017; Zhang et al., 2024) and aquatic plants (Braun et al., 2018; Lingott et al., 2016; Zocher et al., 2022). However, a number of

processes can degrade GBCA chelates, including bacterial activity, UV photo-oxidation (Alvarez-Aguinaga et al., 2022; Birka et al., 2016a) and transmetallation, i.e. the competition for the ligand with other strongly binding metals (Schijf and Christy, 2018). While Möller and Dulski (2010) did not find evidence for significant transmetallation that may cause a release of ionic Gd^{3+}, Le Goff et al. (2019) reported that the GBCAs in coastal seawaters in Bay of Brest, Brittany, France, are partially degraded and that the labile anthropogenic Gd^{3+} ions, most likely released from linear compounds, are readily incorporated into the soft tissue of mussels and limpets. Similarly, Castro et al. (2023) recently reported biotic uptake of excess gadolinium in *Mytilus* spp. downstream a GBCA-producing industry plant in southern Norway.

Gadolinium is part of the lanthanide group of elements ("rare earth elements"; chemical elements La to Lu). Due to its same charge and similar ionic radius to Ho, Y is considered a pseudolanthanoid, and together with the lanthanides is commonly referred to as "rare earths and yttrium" (REY). The REY share similar physico-chemical properties and are thus regarded as a group of "geochemical siblings" with coherent behavior in most natural systems. With the exception of Ce and Eu, the REY are strictly trivalent and due to their high ionic charge and small ionic radii, they are very particle-reactive, i.e. they have a strong tendency to be removed from the truly dissolved REY pool in natural waters by preferentially binding to active surface sites of nanoparticles

and colloids (NPCs) and larger particles. In most surface waters, the natural dissolved REY concentrations are thus low, i.e. in the ng kg^{-1} range. Large-scale removal of particle-reactive elements from estuarine waters is common, with removal rates of up to 97 % from the dissolved load (Sholkovitz, 1993) due to salt-induced particle aggregation, coagulation and subsequent sedimentation (Elderfield et al., 1990; Merschel et al., 2017; Sholkovitz, 1993; Tepe and Bau, 2016). Dissolved REY concentrations in seawater, therefore, are even lower and in the pg kg^{-1} range (De Baar et al., 1985). This estuarine mixing is one of the main processes that control REY input into the oceans. While the particle-reactive REY are associated with NPCs, the strongly complexed anthropogenic Gd from the GBCA can be regarded as truly dissolved, i.e. it is not associated with NPCs (Kulaksiz and Bau, 2007). Under certain circumstances, even particle-reactive elements like the geogenic REY, however, behave conservatively upon estuarine mixing, as was reported, for example, for organic particle-rich rivers such as some boreal rivers in NW Russia (Pokrovsky and Schott, 2002), the Rio Negro (Merschel et al., 2017) or the Rio Pará Bay in Brazil (Xu et al., 2023). This remarkably different behavior of the REY is sometimes attributed to strong complexation of trace elements by dissolved organic matter (DOM) such as fulvic or humic acids (e.g., Merschel et al., 2017). Similar to natural organic complexes, the highly stable organic GBCAs that are employed for MRI scans, can therefore bypass the natural estuarine REY "trap". Although the chemical form of GBCAs has changed over time from linear GBCAs in the 1990s to today mainly macrocyclic GBCAs, the high chemical stability of these complexes effectively enables their transport across estuaries into the open ocean. Kulaksiz and Bau (2007), therefore, suggested that anthropogenic Gd anomalies can be utilized as a pseudo-natural far-field tracer for truly dissolved waste water-derived substances (WWDS) in seawater.

Here, we present a detailed study on the REY inventory, including Gd, of the southern and central North Sea, with the German Bight, the German Exclusive Economic Zone (EEZ) part of the Dogger Bank, the southern part of Fladen Ground in the British EEZ, and the major Central European rivers Ems, Weser and Elbe that drain into the German Bight. We also discuss our data in the context of recently published REY data for the rivers Rhine and Thames, two of the largest sources of riverine REY to the North Sea. We show that all studied rivers, large parts of the German Bight as far north as the Dogger Bank, and surface waters in the southern part of Fladen Ground (about 200 km east of the British coastline) show evidence of microcontamination with GBCAs and, therefore, possibly with other persistent WWDSs that behave similarly.

2. Materials and methods

2.1. Samples

Water samples were taken amidst the COVID-19 pandemic in December 2020 during R/V Meteor research cruise M169 (TRAM "Tracing geogenic and anthropogenic critical high-technology metals in the southern North Sea"; Koschinsky et al., 2020). Additional water samples in the open North Sea from the area of Fladen Ground and around Heligoland were obtained during a later R/V Alkor research cruise AL575 in June and July 2022.

2.1.1. Rivers

Three river water samples were taken by a "land-based" team from the Ems, Weser and Elbe rivers, respectively, at the same time when the North Sea and the estuaries were sampled during cruise M169 on December, 7th (Ems), 18th (Elbe) and 23rd (Weser) 2020. The sampling localities were chosen upstream from the estuaries with no tidal influence. The samples have low conductivities of <5 PSU and pH values between 7.6 and 8.1. The southern North Sea is also influenced by a significant influx of freshwater from the Rhine-Meuse delta and the Thames estuary. Therefore, our data set on river waters is complemented by recent data from samples from the lower reaches of the River Thames

downstream of London, U.K. (Alemu et al., 2024), and the Rhine River, downstream of Bonn, Germany (Zhang et al., 2024).

2.1.2. German Bight and North Sea

From the German Bight and beyond, a set of 98 water samples from the southern and central North Sea were analyzed (Fig. 1). The samples were taken during cruise M169 with R/V Meteor in the areas of the North Frisian and East Frisian Islands, around Heligoland and towards the Dogger Bank. Additional samples were taken during R/V Alkor cruise AL575 in the area around Helgoland and in the open North Sea (between Edinburgh, UK, and Kristiansand, Norway) in the southern part of Fladen Ground. Sampled water depths range from 1.5 m to 148 m. While surface waters (upper 10 m) were sampled at each station, additional deeper waters were also sampled at some locations (deeper parts of the North Sea, e.g., stations 067GoFlo, 140GoFlo, 159GoFlo, and others). Salinity was in the range of 22.1 to 33.8 PSU. The pH values cover only the small range from 7.9 to 8.2.

2.2. Methods

2.2.1. Water sampling and filtration

Seawater: The coastal and high-salinity seawater samples were taken with 5 L-sized Go-Flo bottles (Ocean Test Equipment, Inc.) which were deployed with a metal-free 8 mm Kevlar wire mounted at R/V Meteor. The Go-Flo bottles, made from PVC and coated with PTFE, were cleaned prior to the cruise with alkaline detergent, 0.1 M HCl and de-ionised (DI; 18.2 MΩ•cm) water. Between the stations, the GoFlo bottles were rinsed with DI water. The bottles had both ends open when entering the water and were closed with a weight messenger at the desired depth. At each CTD station, we used two GoFlo bottles. After retrieval, the outlets were rinsed thoroughly with DI water, and the first ~0.5 L of the sample were used to rinse the outlet and the tubings and were then discarded. A tubing with a 0.8/0.2 μm AcroPak PES membrane filter capsule (Pall®) was attached to the outlet and the filtered water samples were filled into acid-cleaned LDPE bottles. For details, please refer to the cruise report (Koschinsky et al., 2020). Water parameters (pH, salinity, conductivity) were taken immediately prior to the filtration of the water samples on separate aliquots. The water samples were acidified under a portable HEPA filtered ISO class 5 laminar flow bench (Colandis, Germany) to pH 1.8 using ultrapure HCl (Roth, 34 %) immediately after sampling and filtration.

Low salinity seawater and river water: Due to the high particle load of the rivers, the GoFlo bottles used onboard often malfunctioned as the particles (mainly of sand and silt size) tended to block the closing mechanism. Therefore, some water samples with lower salinity (labelled with 'pump') were taken on-board with a custom-built tubing construction. A 15 m long section of a laboratory polymer tubing was cleaned by continuously rinsing with 6 M HCl and DI water before it was attached to a Kevlar rope with cable ties. The rope (with a plummet attached at one end) was lowered into the water at a minimum distance of 2 m from the ship until it reached the desired sampling depth before water was continuously pumped through the tubing with the help of a peripump. The first liters were discarded. A 0.8/0.2 μm AcroPak PES membrane filter capsule (Pall®) was attached to the tubing, and the samples were directly filtered into acid-cleaned LDPE sample bottles. Water parameters (pH, salinity, temperature) were taken with a portable multimeter immediately after filtration of the water samples on separate aliquots. The river water endmember samples were taken directly into acid-cleaned 1000 mL LDPE bottles by the land-based team and filtered with 0.2 μm cellulose acetate filters and a vacuum filtration unit. All filtered river water samples were acidified under a portable clean air bench to pH 1.8 using ultrapure HCl (Roth, 34 %) immediately after sampling and filtration.

2.2.2. Analytical methods

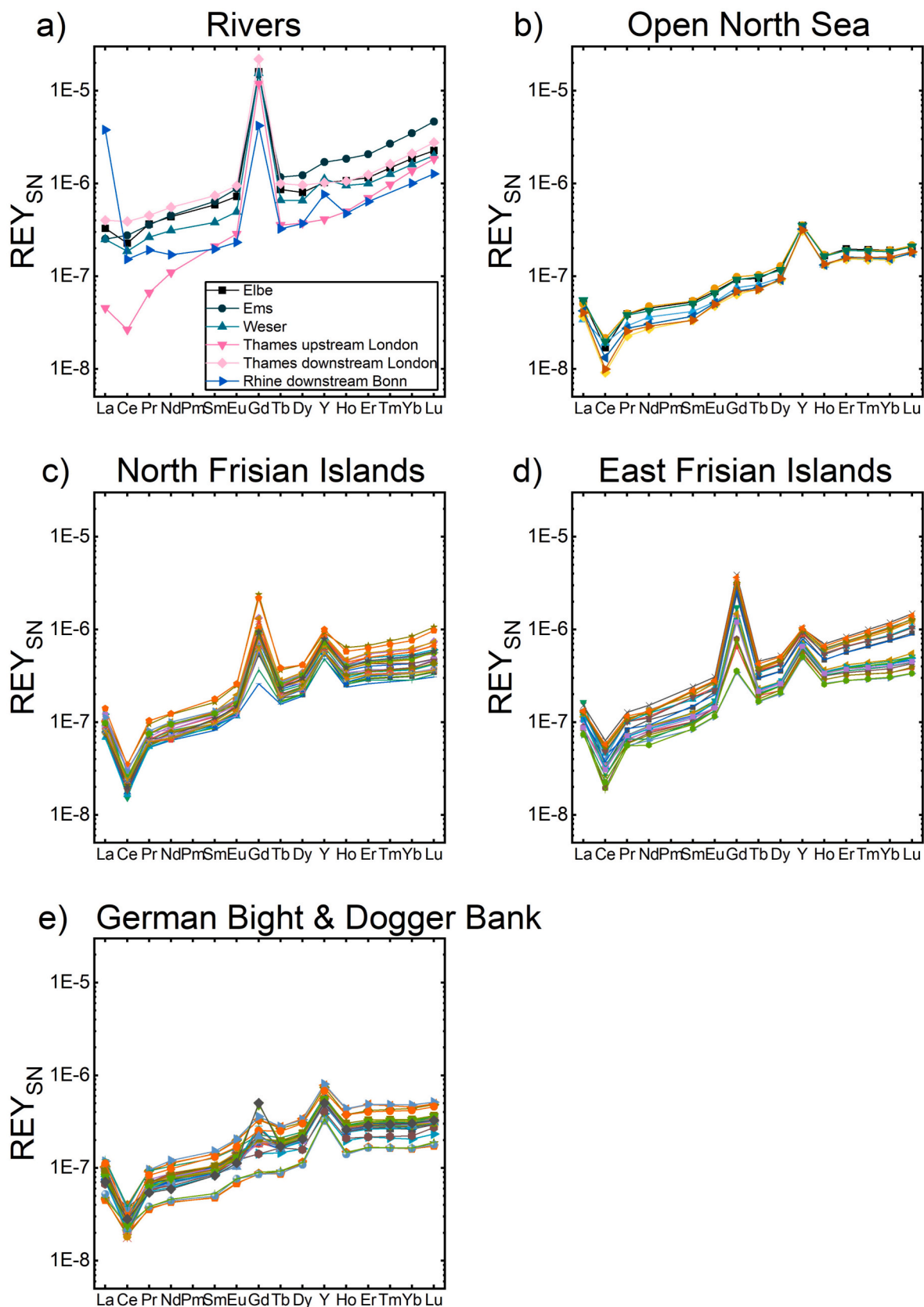To avoid contamination in the home laboratory, all sample handling

Fig. 2. a-e: REY$_{SN}$ plots of (a) river water endmembers (Rhine River data from Zhang et al., 2024; River Thames data from Alemu et al., 2024), (b) samples from the open North Sea (ALK575 cruise), samples from the areas around the (c) North Frisian and (d) East Frisian Islands and from (e) the German Bight towards Dogger Bank. Note the prevailing Gd anomalies present in the majority of the investigated water samples.

and method solution handling was performed in an HEPA filtered ISO class 5 laminar flow bench (Colandis, Germany) in the Geochemistry laboratory of the Department of Marine Resource Exploration at BGR. The cleaning procedure for all plastic equipment (HDPE and LDPE bottles) has been adopted in slightly modified form from the GEO-TRACES trace metal cleaning protocol (see Appendix A1).

2.2.2.1. Water analysis with seaFAST – APEX - ICP-MS/MS. SeaFAST SP2 online preconcentration: The samples were preconcentrated in an automated, commercially available Elemental Scientific seaFAST SP2 system that is equipped with a prepFAST module to allow for autodilution and matrix matching, and with an autosampler in a HEPA-filtered, laminar flow hood. This system utilises two Nobias PA1 resin columns (200 μL) and automatically loads, washes and elutes the analytes with automated syringes in a high-purity PFA environment. The preconcentration factor during the online SeaFAST application is about 15. Details regarding the reagent preparation and the analytical method are provided in Appendix A1.

Reagents: All seaFAST reagents used for this study were of ultra-high purity and were prepared using ultra-pure DI (18.2 MΩ cm^{-1} resistivity) from a Sartorius water purification system. In short, we used a 4 mol L^{-1} ammonium acetate buffer with a pH adjusted to 6.20 ± 0.05, a 5 % HNO$_3$ eluting acid, a HCl pH 1.7 carrier/diluent solution for autocalibration and autodilution, and a 10 % (v/v) NaCl stock solution for matrix matching of all solutions to 3 % NaCl (except for seawater reference materials). Indium (10 μg L^{-1}) was used as an internal standard (IS) during analysis and prepared in 5 % HNO$_3$. All reagents were stored in acid-cleaned Nalgene HDPE or LDPE bottles. For external calibration, a mixed multi-element calibration standard (0.025 μg L^{-1}) was gravimetrically prepared in a dilute HCl matrix (HCl pH 1.7) for each measurement run.

Detection method and evaluation: For the analysis of REY, including Gd, samples were processed in the laboratory of the Geochemistry Research Unit (sub-department "Soil as a Resource – Properties and Dynamics") at BGR with a tandem inductively-coupled plasma mass spectrometer (ICP-MS/MS; Thermo Fisher Scientific iCAP-TQ), that was coupled with the seaFAST SP2 (Elemental Scientific Inc.). To enhance sensitivity, an Apex 2Q desolvating nebulizer (Elemental Scientific Inc.) was used prior to sample introduction into the ICPMS/MS.

Fladen Ground and Dogger Bank

Legend:
- AL575 10ROV 131m
- AL575 01CTD 5-6m
- M169 059GoFlo 8m
- M169 059GoFlo 50m
- NW Atlantic Deep Water (BATS 2000m; van de Flierdt et al. 2012)

Fig. 3. Comparison of seawater REY$_{SN}$ patterns demonstrating the potential presence of small but unquantifiable amounts of anthropogenic Gd in surface water samples from the Dogger Bank (M169 059GoFlo) and south of Fladen Ground (AL575 01CTD) compared to pristine North Atlantic seawater (Van De Flierdt et al., 2012) and the seawater sample AL575 10ROV sampled in the Fladen Ground area at a depth of 131 m. For further discussion see text.

The ICP-MS/MS system was operated in oxygen mode and was tuned to CeO/Ce ratios of around 1 %. The detection of REY mass intensities is based on chromatographic peak integration in the time-resolved signals during the seaFAST preconcentration mode. No interference corrections for the REY were made, as interferences are minimized due to the matrix separation with seaFAST and the use of the oxygen mode in the reaction cell and mass shifts for REY (Appendix Table S4). During the study, both In and Tm were tested as elements for internal standard (IS) correction of the REY data. However, in the course of data evaluation, we noticed a better matching for In-corrected REY data to published reference values and thus decided to use only In-corrected data for the scope of this study. As Tm spikes were tested for internal standardization, the actual Tm concentrations are not reported here, but were modelled instead (see Section 2.2.3).

Limits of quantification (LOQ) are calculated based on ten times the standard deviation of measured acid blanks and provided in appendix table S4.

2.2.2.2. Quality control. For analytical quality control, we used the certified reference materials (CRMs) SLRS-6 and NASS-7 (river water and seawater, respectively; both from National Research Council of Canada), along with a GEOTRACES inter-calibration sample (BATS 2000 m) with community consensus values for REE, that is commonly used as reference standard for REE in seawater. The data are provided in Appendix Table S3 together with a comparison to published literature values. None of the CRMs have certified REY concentration values provided by the issuing organization, and we compared our data to datasets published in the scientific literature. The SLRS-6 data were compared to the datasets of Schmidt et al. (2019), Yeghicheyan et al. (2019), Babechuk et al. (2020), Schmidt et al. (2022), and Ebeling et al. (2022). The NASS-7 data were compared to the published datasets of Schmidt et al. (2022) and Ebeling et al. (2022), and the BATS 2000 m data were compared to van de Flierdt et al. (2012). While most of the datasets were produced with techniques involving offline-matrix separation/preconcentration in combination with different (single quadrupole) ICP-MS techniques, Ebeling et al. (2022) also measured the samples with a combination of a seaFAST SP2 with an ICP-MS/MS.

Published REY concentrations in SLRS-6 are in good agreement with each other (Appendix Table S4). The analytical accuracy in this study is within 5 % for all REY (in comparison with published values by Babe-chuk et al., 2020), the method precision determined from six individual measurement runs is better than 4 % for Pr, Nd, Sm, Dy, Ho, Er, and Yb and better than 6 % for Y, La, Ce, Eu, Gd, Tb, Ho, and Lu. To the best of our knowledge only two studies published REY values for NASS-7 yet (Ebeling et al., 2022; Schmidt et al., 2022) and the analytical accuracy during this study is within 5 % for all REE except for Eu (within 7 %) and Y (within 13 %) in comparison with published data from Ebeling et al. (2022). The method precision is better than 10 % for most elements, except for Eu, Tb, Ho, and Lu (<16 %). The analytical accuracy for the GEOTRACES BATS 2000 m seawater standard is very good and within 5 % for all REE, in comparison with the original study by Van De Flierdt et al. (2012). Yttrium concentrations agree within 11 % with Y concentration in Laukert et al. (2017). The method precision of four individual measurement runs is better than 3 % for most elements, except for Ho, Er, and Yb (<5 %). All CRMs were measured several times during a measurement sequence, and the run precision is usually better than 5 %.

2.2.2.3. Influence of treatment with H_2O_2 and UV on decomposition of Gd-based contrast agents and seaFAST column chemistry. Previous studies using ion exchange columns (Sep-Pak C18 cartridges™, BioRad) loaded with a mixture of ethyl-hexyl-phosphates for offline matrix separation/ REY preconcentration (e.g., Merschel and Bau, 2015; Schmidt et al., 2019) have shown that a quantitative loading of anthropogenic Gd is only ensured by the addition of hydrogen peroxide (H_2O_2) or other strong oxidizers to the sample prior to the column loading step, as this
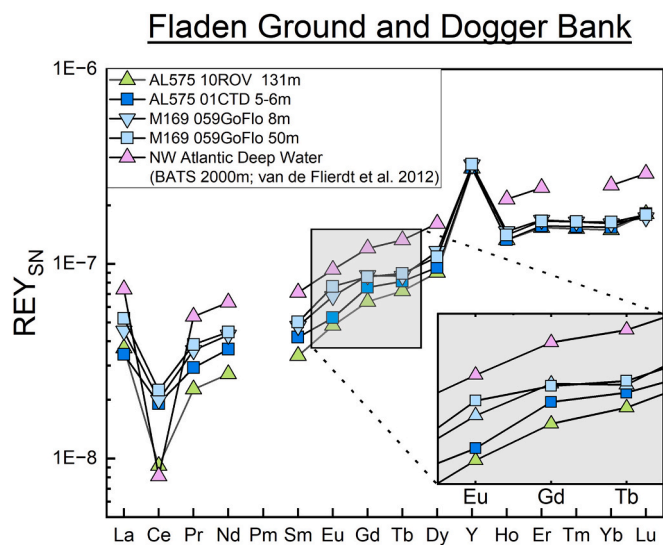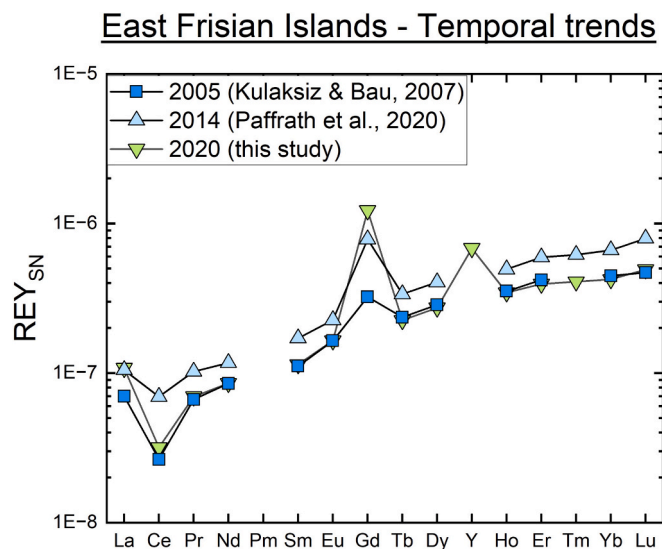
East Frisian Islands - Temporal trends

Fig. 4. REY$_{SN}$ plot of coastal seawater sampled just north of the island of Spiekeroog (from 'East Frisian Islands' subgroup) in comparison to literature data for seawater from a similar location from 2005 (Kulaksiz and Bau, 2007) and 2014 (Paffrath et al., 2020). Note the remarkable similarity of the 2020 pattern with the 2005 data by Kulaksiz and Bau (2007; sample EF5) and the strongly increasing (logarithmic scale!) microcontamination of the German Wadden Sea with anthropogenic Gd.
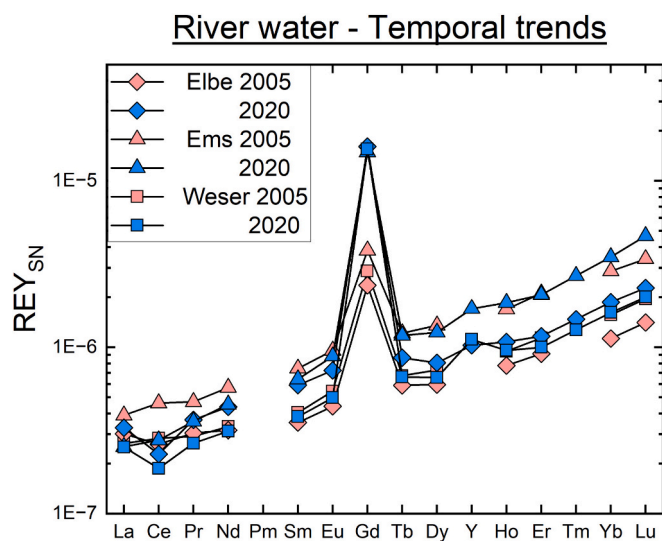
River water - Temporal trends

Fig. 5. REY$_{SN}$ plot of Elbe, Ems and Weser river water samples from 2005 (Kulaksiz and Bau, 2007) and this study. Small variations in overall REY distributions between 2005 and 2020 are possible due to different sampling seasons and different precipitation and discharge rates at the time of sampling. Note the significant increase of anthropogenic Gd microcontamination in all three major rivers since 2005.

facilitates the decomposition of the (bio)chemically inert and stable GBCA compounds. Without the H$_2$O$_2$ step, only up to 50 % of anthropogenic Gd was retained on the C18-ethy-hexyl-phosphate columns, most likely from linear complexes. Hence, this additional step has become a prerequisite for any study that aims at quantifying anthropogenic Gd using this method.

In order to test this for the seaFAST Nobias PA-1 column that was used in the present study, selected seawater and river water samples from the M169 cruise, with various intensities of anthropogenic Gd contamination, were treated with UV or H$_2$O$_2$ in addition to the seaFAST

sample preparation procedure described above. A 10 mL sample aliquot was treated with 0.5 mL of suprapure H$_2$O$_2$ and kept in an oven at 60 °C for three days, together with an untreated aliquot, before the measurement with seaFAST-ICP-MS/MS. Additional aliquots were digested with UV light at 70 °C. Comparison of the Gd yields between H$_2$O$_2$-treated, UV-treated and untreated samples revealed only minor differences (Appendix Figs. 1 and 2). Gadolinium recovery in the untreated samples was in the range of 94 to 105 % relative to the H$_2$O$_2$-treated counterparts (mean: 97 %; $n = 8$), which is close to the analytical uncertainty of the Gd measurements.

2.2.3. Reporting of REY data and calculation of anomalies

Rare earths and yttrium concentrations (Appendix Table S2) are normalized to European Shale (EUS; Bau et al., 2018) and are then referred to as REY$_{SN}$ (e.g., Figs. 2–5). These normalized data are provided in Appendix Table S3. Geogenic ('background') Gd concentrations, [Gd]* or [Gd]$_{geo}$, are calculated based on the shale-normalized concentrations of Eu and Nd following Eqs. 1 and 2 in Kulaksız and Bau (2013):

$$log\ Gd^{*}_{SN} = (4 \times log\ Eu_{SN}–log\ Nd_{SN}/3 \tag{1}$$

$$Gd^{*} = Gd^{*}_{SN}\ x\ [Gd]^{EUS} \tag{2}$$

There are numerous mathematical approaches reported in the literature to constrain Gd* from normalized data. We emphasize that extrapolation from Nd over Eu to constrain Gd* is a valid approach *only* if the samples do not show Eu anomalies in normalized patterns and *only* if BaO interferences on Eu are absent or corrected by technical (matrix separation with IX columns, use of collision or reaction cell gases during ICP-MS analysis) or mathematical means (oxide yield determination and correction; Dulski, 1994) or, ideally, a combination of both.

The concentration of anthropogenic Gd can be quantified from Gd* as the difference between the measured total Gd concentration and the calculated geogenic Gd concentration from Eq. 3 (Schmidt et al., 2019):

$$[Gd]_{anth} = [Gd_{measured}]–Gd^{*} \tag{3}$$

Because of the general uncertainty in the analytical methodology and the small natural positive Gd anomaly (due to REY speciation) of seawater (e.g., North Atlantic seawater; Fig. 3), we applied a general cut-off of 5 % for anthropogenic Gd, i.e. water samples that have been calculated to contain ≤5 % anthropogenic Gd relative to total dissolved Gd are considered devoid of anthropogenic Gd regardless of any small positive Gd anomalies visible in normalized REY patterns.

Thulium was used as an internal standard element for the REY preconcentration and thus Tm concentrations in the samples were calculated (Tm*) from shale-normalized data by interpolation between Er and Yb following eq. 4 (adapted from Kulaksız and Bau, 2011):

$$Tm_{interpolated} = Tm_{SN}\ x\ 10^{\char`^}(0.5\ log\ Er_{SN} + 0.5\ log\ Yb_{SN}) \tag{4}$$

3. Results

To facilitate comparison, the river and seawater samples are divided into five subgroups based on their respective sampling localities (see Figs. 1 and 7): (a) river water ('River waters'), (b) North Sea water from between the German Bight and the Dogger Bank ('German Bight + Dogger Bank'), (c) North Sea water from close to the North Frisian Islands including Heligoland ('North Frisian Islands') and (d) East Frisian Islands ('East Frisian Islands'), and (e) North Sea water from the southern Fladen Ground ('Open North Sea', British EEZ). Summary statistics of all subgroups are presented in Table 1. Analytical data including calculated data for anthropogenic Gd are compiled in Appendix Tables S2 and S3. The highest concentrations of geogenic dissolved REY ($\sum$REY$_{geo}$ without Gd$_{anth}$) are found in the Ems, Weser and Elbe rivers with an average $\sum$REY$_{geo}$ concentration of 125.49 ng kg^{-1}. The lowest $\sum$REY$_{geo}$ concentrations occur in the seawater samples from

Table 1
Summary statistics of the samples as divided by subgroups presented in Fig. 1.

| Group	n	Salinity [PSU]	$\sum$REY [ng kg^{-1}]		Anthropogenic Gd [ng kg^{-1}]		Geogenic REY [ng kg^{-1}] ($\sum$REY-Gd$_{anth}$)		Gd$_{anth}$ [%]		Gd$_{anth}$/$\sum$REY *100 [%]
		Mean ± RSD	Mean ± RSD	Median	Mean ± RSD	Median	Mean ± RSD	Median	Mean ± RSD	Median	
Ems, Elbe and Weser rivers	3	<5	218.33 ± 9 %	214.42	92.84 ± 4 %	94.72	125.49 ± 19 %	118.05	95 ± 2 %	95 %	42.53 %
German Bight + Dogger	37	33.06 ± 1 %	32.77 ± 21 %	32.42	0.40 ± 123 %	0.24	32.37 ± 20 %	31.75	15 ± 78 %	15 %	1.21 %
North Frisian Islands + Heligoland	30	31.58 ± 5 %	44.23 ± 22 %	42.45	4.59 ± 55 %	4.34	39.64 ± 19 %	38.6	76 ± 14 %	79 %	10.38 %
East Frisian Islands	24	28.42 ± 14 %	58.64 ± 32 %	53.23	10.86 ± 60 %	8.86	47.78 ± 26 %	44.37	83 ± 6 %	86 %	18.51 %
Open North Sea	7	34.03 ± 1 %	18.80 ± 11 %	17.75	0.07 ± 0.33 %	0.08	18.73 ± 11 %	17.65	14 ± 26 %	13 %	0.39 %
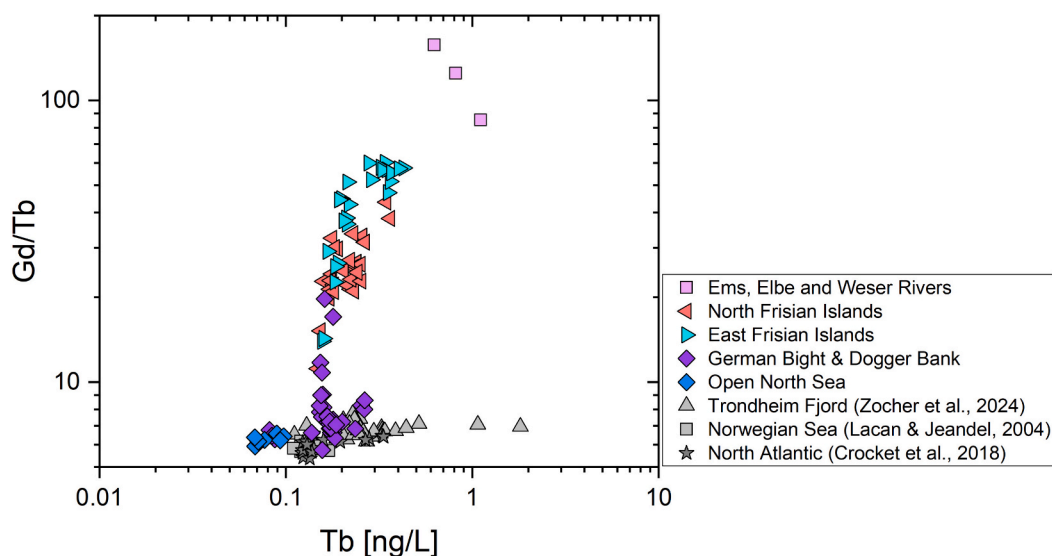
Fig. 6. Terbium concentrations (in ng/L) plotted against Gd/Tb elemental ratios in the studied water samples in comparison to literature data (Trondheim Fjord: 0.2 µm-filtered, Zocher et al., 2024; Norwegian Sea: Stations 23 and 25, unfiltered, Lacan and Jeandel, 2004; North Atlantic: Stations O and P, 0.4 µm-filtered, Crocket et al., 2018).

the British EEZ with an average of 18.7 ng kg^{-1}. The average $\sum$REY$_{geo}$ concentration in the German Bight and Dogger Bank is 32.37 ng kg^{-1}. The North Sea water off the North and East Frisian Islands is slightly enriched with average $\sum$REY$_{geo}$ concentrations of 39.6 and 47.8 ng kg^{-1}, respectively. The REY$_{SN}$ patterns of North Sea water from the British EEZ show REY$_{SN}$ patterns typical of pristine seawater with a small positive La$_{SN}$ anomaly, a negative Ce$_{SN}$ anomaly, a small positive Gd$_{SN}$ anomaly and strong Y—Ho fractionation resulting in a large positive Y$_{SN}$ anomaly (Fig. 2e). Although the absolute REY concentrations differ between the river waters and the North Sea waters, their REY$_{SN}$ patterns are remarkably similar, with a steady increase from the LREY towards the HREY (Fig. 2). The REY$_{SN}$ patterns show large positive Gd$_{SN}$ anomalies of up to 1.5 orders of magnitude in the river waters and up to about one order of magnitude in water samples from off the Frisian Islands, the German Bight and the Dogger Bank. As seen in the REY$_{SN}$ patterns in Fig. 4 and in the map in Fig. 7, even North Sea water from the Dogger Bank further away from the German Bight shows slightly elevated Gd/Tb ratios compared to the apparently most-pristine (in terms of anthropogenic Gd) deep-water sample from southern Fladen Ground in the "open" North Sea, possibly due to the presence of very small amounts of anthropogenic Gd. The Tb vs Gd/Tb graph in Fig. 6 also shows a continuous trend between the Gd$_{anth}$-rich rivers and the pristine Open North Sea samples, with most coastal and German Bight waters plotting in between. This suggests that seawater in the study area

of the German Bight and along the Frisian coastlines is a mixture of apparently pristine North Sea water (ultimately derived from North Atlantic seawater) and Gd-microcontaminated river water. Interestingly, this relationship is unrelated to the salinities of the water samples, which are close to seawater salinity for the majority of samples from the German Bight (viz. Fig. 1).

The fraction of the anthropogenic Gd in the total measured Gd as calculated following Eqs. 1 to 3 (Fig. 7) are highest in the river waters with an average concentration of 92.84 ng kg^{-1} (95 % of the total dissolved Gd load and 42.5 % of the total dissolved REY inventory; Table 1). The waters around the East and North Frisian Islands have average anthropogenic Gd concentrations of 10.9 and 4.6 ng kg^{-1}, respectively. This amounts to 84 % and 77 %, respectively, of the total dissolved Gd load and 18.5 % and 10.4 %, respectively, of the total dissolved REY inventory, respectively. The lowest amounts of anthropogenic Gd are found in the area of the German Bight and the Dogger Bank (0.4 ng kg^{-1}, amounting to 23 % of total dissolved Gd and 1.2 % of total dissolved REY), and in the area of southern Fladen Ground in the British EEZ (0.07 ng kg^{-1}; 14 % of total Gd and 0.38 % of total dissolved REY). The strongest contamination is observed in the rivers, where contrast agent-derived Gd clearly dominates total dissolved Gd (~93–97 %; Table S3) and even dominates the total dissolved REY of the waters (mean: 43 %, Table 1). Towards the Dogger Bank and around the North and East Frisian Islands, the amounts of anthropogenic Gd
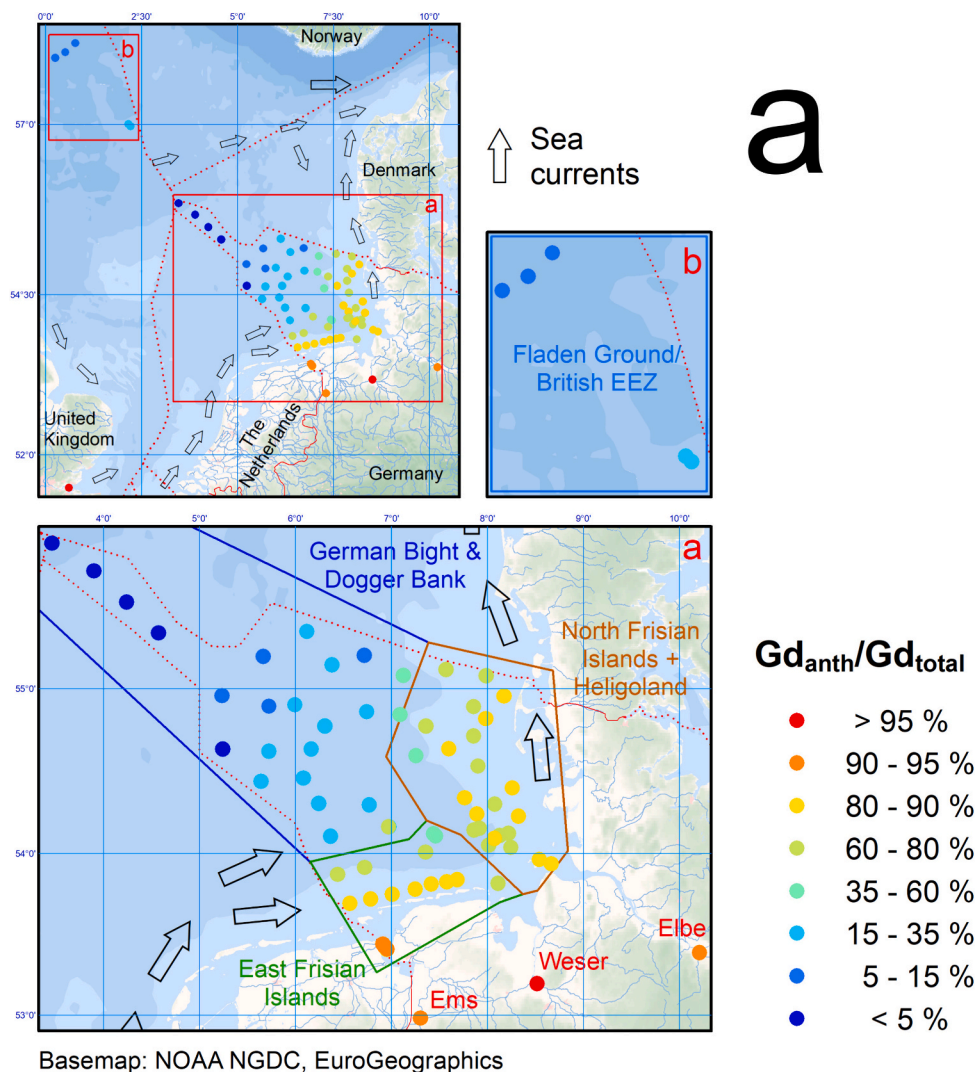
Fig. 7. Maps of the study area with (a) anthropogenic Gd as a share of total Gd (in %), (b) anthropogenic Gd as a share of total REY (in %), and (c) concentrations of anthropogenic Gd (in ng kg^{-1}).

decrease due to mixing (i.e. dilution) with less or un-contaminated seawater, although a significant contamination (60–90 % anthropogenic Gd relative to total dissolved Gd) can still be observed.

4. Discussion

4.1. Riverine input of anthropogenic Gd into the southern North Sea

All available REY data for the lower reaches of the rivers Thames, Rhine, Ems, Weser and Elbe suggest that these rivers carry large amounts of anthropogenic Gd (and potentially other WWDS) into the southern North Sea. The concentration of anthropogenic Gd increased significantly over a time span of only fifteen years. Kulaksız and Bau (2007), for example, reported in their 2005 dataset anthropogenic Gd concentrations of 14.9 ng kg^{-1} (Ems), 24.2 ng kg^{-1} (Elbe) and 18.2 ng kg^{-1} (Weser), respectively. The data we provide here reveals that until 2020, a significant increase by a factor of up to 6.5 with maximum anthropogenic Gd concentrations ranging from 87.4 ng kg^{-1} to 96.4 ng kg^{-1} had occurred in these three rivers (Fig. 5). This is likely a minimum increase, as the samples were taken amid the COVID-19 pandemic during which the number of MRI scans and hence the use of GBCAs had (temporarily) decreased (e.g., Pereto et al., 2023; Krohn et al., 2024),

because hospital occupation was kept at a minimum to free capacity for COVID-19-infected patients. For the Rhine River and the Rhine-Meuse delta, large data sets on anthropogenic Gd contamination have been compiled over the past twenty years or more. Kulaksız and Bau, 2011 reported 25 ng kg^{-1} in the Rhine River near Xanten, Germany. For the Rhine-Meuse delta, in an investigation covering several seasons of 2010, Klaver et al. (2014) reported anthropogenic Gd concentrations of 30–80 ng kg^{-1} in the (Dutch parts of the) Rhine River, 50–80 ng kg^{-1} in the Ijssel River and 30–60 ng kg^{-1} in the Meuse River. Most recent data from January 2020 by Zhang et al. (2024) for the Rhine River close to Bonn, Germany, shows 26.6 ng kg^{-1} anthropogenic Gd, an increase by 37 % from 2013 (19 ng kg^{-1}; Kulaksız and Bau, 2013) at a similar location. Another major river that drains into the North Sea is the River Thames. Data reported for the River Thames in 2009 (Kulaksız and Bau, 2011) showed comparatively low anthropogenic Gd concentrations of only 2.7 ng kg^{-1}, but by 2023 the concentration in the River Thames downstream from London had increased almost 50-fold to 130 ng kg^{-1} (Alemu et al., 2024). A conservative estimate based on the average daily discharge rates of the four rivers Rhine, Ems, Weser and Elbe at the time of sampling (data from "Wasserstraßen- und Schifffahrtsverwaltung des Bundes", WSV, provided by the "Bundesanstalt für Gewässerkunde", BfG, Koblenz, Germany) and the reported anthropogenic Gd
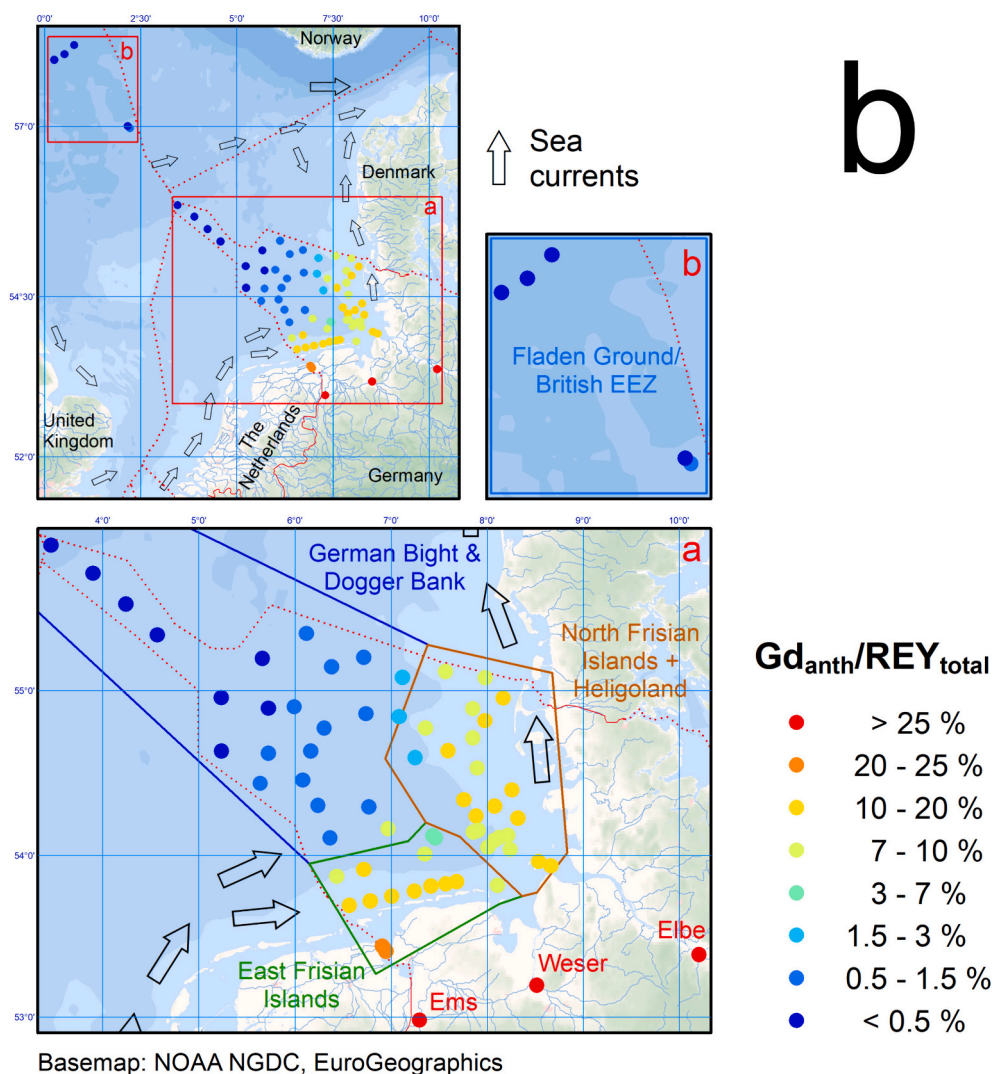
Fig. 7. (*continued*).

concentrations in the rivers suggests a total flux of ca. 8 kg anthropogenic Gd per day (at the day of sampling) into the North Sea via these four rivers alone. This amounts to an estimated input of ~28 kg GBCA per day (simplified, assuming that Dotarem© with a molar mass of 558.7 g/mol is the prevalent GBCA). Note, however, that these calculations are prone to significant error as the rivers were not sampled on the same day and as there are additional points of waste water discharge downstream the river sampling sites that add anthropogenic Gd to the estuary and hence the North Sea (e.g., Hamburg and Cuxhaven for the Elbe River). However, based on these very rough estimates, it is reasonable to assume that significant amounts of GBCAs, in the range of several tonnes per year, are introduced into the southern North Sea by just the Rhine, Ems, Weser and Elbe rivers.

Several studies have shown that the anthropogenic Gd from GBCAs behaves conservatively in estuaries as it is not associated with riverine NPCs and hence not removed from the water during estuarine aggregation of these ultrafine particles (e.g., Kulaksiz and Bau, 2007; Hatje et al., 2016). Hence, trapping of the GBCAs with their anthropogenic Gd in the estuaries of the rivers Thames, Rhine, Ems, Weser and Elbe should be very minor, explaining the widespread Gd (micro)contamination of the southern North Sea.

4.2. Anthropogenic Gd as a far field tracer for persistent wastewater-derived substances in the North Sea

Our results confirmed the notion that major parts of the UNESCO world heritage site of the Wadden Sea, including the areas off the tourism hotspots of the North Frisian Islands of Sylt, Foehr, Amrum, and Pellworm, and the East Frisian Islands of Borkum, Juist, Norderney, Baltrum, Langeoog, Spiekeroog, and Wangerooge are (micro)contaminated with GBCA. In previous studies (Kulaksiz and Bau, 2007; Paffrath et al., 2020) surface water just north of Spiekeroog was found to carry 0.59 ng kg^{-1} (2005) and 3.2 ng kg^{-1} (2014) of anthropogenic Gd, respectively. Our recent data reveals that the anthropogenic Gd concentration off Spiekeroog had increased to 6.4 ng kg^{-1} by 2020, i.e. 11-fold and 2-fold, respectively, compared to 2005 and 2014 (Fig. 5).

Screening large parts of the southern North Sea with regard to the REY distribution and using anthropogenic Gd as a proxy for WWDS allows to track their dispersion by the major water currents in the German Bight (Figs. 2 and 7). The major water masses in the southern North Sea flow eastwards along the Dutch and German coasts after having entered the North Sea via the Strait of Dover in the west and having mixed with water masses coming from the north along the U.K. coast (Turrell, 1992). Finally, these water masses turn northwards along the Danish coast in the east (OSPAR Commission, 2000; Turrell, 1992). This flow regime is also reflected in the distribution of anthropogenic Gd (Fig. 7).
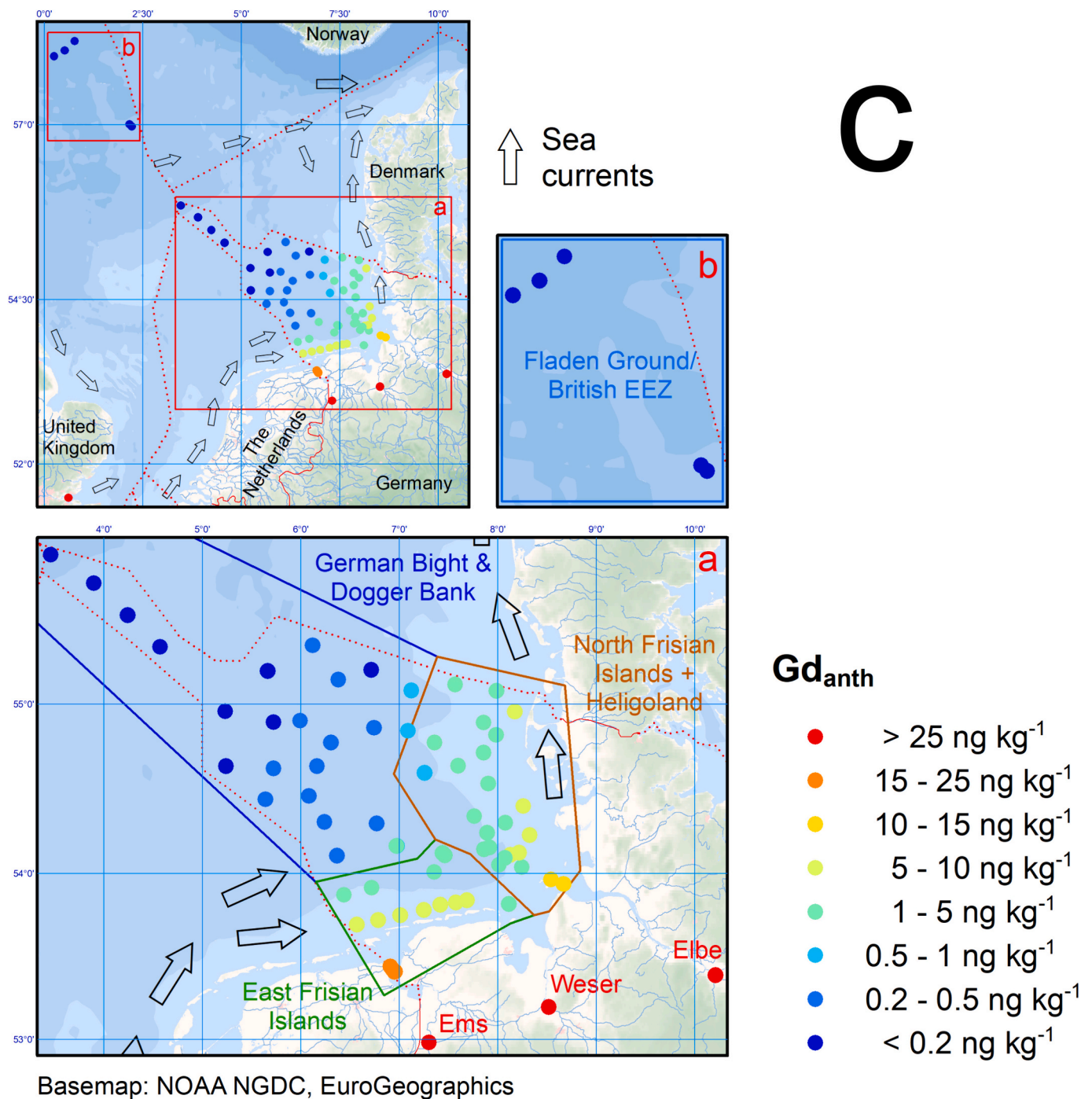
Fig. 7. (*continued*).

The high anthropogenic Gd concentrations in North Sea water observed as far west as the westernmost East Frisian Islands (Borkum, Juist; 3–8 ng kg^{-1}) probably do not solely result from the water discharge of the Ems River with 87 ng kg^{-1} anthropogenic Gd, but also from anthropogenic Gd input from the Rhine River (26.6 ng kg^{-1} anthropogenic Gd, but higher discharge) and maybe the highly contaminated River Thames (130 ng kg^{-1} anthropogenic Gd) with their densely populated catchments. Further east, additional contributions from the Weser and Elbe rivers add to the anthropogenic Gd load of the southern North Sea (Fig. 7), where the water currents transport the GBCA-bearing water masses further north towards the Danish Coast. From here, the water masses may enter the Baltic Sea via the Jutland Coastal Current and the Norwegian Sea via the Norwegian Coastal Current. Zocher et al. (2024)

studied coastal waters in the Trondheimfjord and reported small amounts of anthropogenic Gd in Norwegian coastal waters. They showed that this anthropogenic Gd is not derived from local sources in the wider Trondheim area and suggested input of anthropogenic Gd transported with the Norwegian Coastal Current from further south towards the Norwegian Sea. Our data appears to be the "missing link", as we show that significant amounts of anthropogenic Gd are, indeed, exported from the southern North Sea northwards with the Jutland Coastal Current. Considering the current regime, significant amounts are probably also exported from the North Sea towards the Baltic Sea via the Skagerrak and Kattegat. However, a similarly detailed study on Gd micro-contamination in the Skagerrak, Kattegat and the Baltic Sea has not been conducted yet, despite significant additional evidence for

similar GBCA (micro)contamination originating from rivers that drain into the Baltic Sea (Alemu et al., 2024; Wysocka et al., 2023; Zocher et al., 2022).

4.3. Anthropogenic Gd as a sensitive, yet robust far-field tracer for persistent and mobile wastewater-derived substances

As long as the GBCAs are stable and not decomposed, the highly toxic Gd^{3+} ions are contained within the safe structure of the ligand and do not, to current knowledge, pose any significant threat to freshwater or marine organisms. However, due to their inert and mobile character, the presence of GBCAs in a water-mass may suggest the co-presence of other persistent, but potentially toxic, WWDS (such as "Persistent, Mobile and Toxic" (PMT) substances and "very Persistent and very Mobile" (vPvM) substances; see Hale et al., 2020). This has been demonstrated for anthropogenic Gd and natural and synthetic estrogens (Morteani et al., 2006) and is very likely for other pharmaceutical or personal care products and their metabolites (e.g., cocaine, cannabis, endocrine disruptors and non-steroidal anti-inflammatory drugs like ibuprofen or diclofenac). However, in contrast to these (micro)contaminants, the analytical work involved in the determination of anthropogenic Gd is relatively straightforward and with the help of automated preconcentration systems more time- and cost-effective than the screening of water samples for individual (organic) substances (e.g., Krohn et al., 2024). Therefore, we encourage that anthropogenic Gd is, due to its chemical robustness and conservative behavior, and due to the sensitivity of the analytical method, tested in follow-up studies as a screening proxy ('waste marker') in coastal seawater samples for a range of PMT and vPvM substances which fall, for example, under the framework of the European Union REACH regulation (Registration, Evaluation, Authorisation and Restriction of Chemicals).

5. Conclusions

Elevated concentrations of anthropogenic Gd related to GBCAs were found in the rivers Ems, Weser and Elbe. These rivers effectively transport the contrast agents into the Wadden Sea and the German Bight. Anthropogenic Gd – and probably other persistent WWDS – are, as a consequence, now present in large parts of the southern North Sea. Their dispersion mimics the overall riverine input and the major current systems that operate in the southern North Sea. The anthropogenic Gd anomalies, despite considerable dilution, allow to effectively trace water masses and currents and to reconstruct the mixing of different water masses in the marine environment, thereby allowing to track the dispersion of WWDS from the rivers into the open sea. The concentrations found in the river systems as well as in the southern North Sea are not (eco)toxicologically relevant yet. However, due to its chemical robustness and the low detection limits of the current analytical methods, anthropogenic gadolinium might be used as a sensitive screening proxy (waste marker) for potentially hazardous, persistent pharmaceutical compounds and other WWDS in natural waters in addition to its application as a (anthropogenic) water mass proxy.

CRediT authorship contribution statement

Dennis Kraemer: Writing – original draft, Visualization, Validation, Supervision, Resources, Project administration, Methodology, Investigation, Funding acquisition, Formal analysis, Data curation, Conceptualization. **Katja Schmidt:** Writing – original draft, Visualization, Validation, Project administration, Methodology, Investigation, Funding acquisition, Formal analysis, Data curation, Conceptualization. **Franziska Klimpel:** Writing – original draft, Methodology, Investigation, Formal analysis, Data curation. **Uwe Rauch:** Writing – original draft, Visualization, Methodology, Investigation, Formal analysis, Data curation. **David M. Ernst:** Visualization, Validation, Investigation, Formal analysis, Data curation. **Sophie A.L. Paul:** Writing – original

draft, Validation, Investigation, Funding acquisition, Data curation, Conceptualization. **Matthias Haeckel:** Writing – original draft, Resources, Methodology, Investigation. **Andrea Koschinsky:** Writing – review & editing, Writing – original draft, Project administration, Funding acquisition, Data curation, Conceptualization. **Michael Bau:** Writing – review & editing, Writing – original draft, Validation, Supervision, Resources, Project administration, Funding acquisition, Data curation, Conceptualization.

Declaration of competing interest

Andrea Koschinsky reports financial support was provided by German Research Foundation. Michael Bau reports financial support was provided by European Union. Michael Bau reports financial support was provided by Research Council of Norway. If there are other authors, they declare that they have no known competing financial interests or personal relationships that could have appeared to influence the work reported in this paper.

Data availability

Data will be made available on request.

Appendix A. Supplementary data

Supplementary data to this article can be found online at https://doi.org/10.1016/j.marpolbul.2024.116794.

References

Alemu, A.K., Zhang, K., Klimpel, F., Zocher, A.-L., Bau, M., 2024. The inventory of geogenic and anthropogenic rare earth elements and yttrium in major European Rivers and lakes. In: EU-ITN PANORAMA Annual Meeting. Rennes, France.

Alvarez-Aguinaga, E.A., Elizalde-González, M.P., García-Díaz, E., Sabinas-Hernández, S. A., 2022. UV-light-driven conversion of gadoterate meglumine: insight into the photocatalyst's influence on conversion pathway, transformation products, and release of toxic ionic gadolinium. Catal. Commun. 172, 106544.

Babechuk, M.G., O'Sullivan, E.M., McKenna, C.A., Rosca, C., Nägler, T.F., Schoenberg, R., Kamber, B.S., 2020. Ultra-trace element characterization of the central Ottawa River basin using a rapid, flexible, and low-volume ICP-MS method. Aquat. Geochem. 26, 327–374.

Barrat, J.-A., Chauvaud, L., Olivier, F., Poitevin, P., Bayon, G., Salem, D.B., 2022. Rare earth elements and yttrium in suspension-feeding bivalves (dog cockle, Glycymeris

glycymeris L.): accumulation, vital effects and pollution. Geochim. Cosmochim. Acta 339, 12–21.

Bau, M., Dulski, P., 1996. Anthropogenic origin of positive gadolinium anomalies in river waters. Earth Planet. Sci. Lett. 143, 245–255.

Bau, M., Knappe, A., Dulski, P., 2006. Anthropogenic gadolinium as a micropollutant in river waters in Pennsylvania and in Lake Erie, northeastern United States. Chem. Erde 66, 143–152. https://doi.org/10.1016/j.chemer.2006.01.002.

Bau, M., Schmidt, K., Pack, A., Bendel, V., Kraemer, D., 2018. The European shale: an improved data set for normalisation of rare earth element and yttrium concentrations in environmental and biological samples from Europe. Appl. Geochem. 90, 142–149. https://doi.org/10.1016/j.apgeochem.2018.01.008.

Birka, M., Wehe, C.A., Telgmann, L., Sperling, M., Karst, U., 2013. Sensitive quantification of gadolinium-based magnetic resonance imaging contrast agents in surface waters using hydrophilic interaction liquid chromatography and inductively coupled plasma sector field mass spectrometry. J. Chromatogr. A 1308, 125–131.

Birka, M., Roscher, J., Holtkamp, M., Sperling, M., Karst, U., 2016a. Investigating the stability of gadolinium based contrast agents towards UV radiation. Water Res. 91, 244–250.

Birka, M., Wehe, C.A., Hachmöller, O., Sperling, M., Karst, U., 2016b. Tracing gadolinium-based contrast agents from surface water to drinking water by means of speciation analysis. J. Chromatogr. A 1440, 105–111.

Braun, M., Zavanyi, G., Laczovics, A., Berényi, E., Szabó, S., 2018. Can aquatic macrophytes be biofilters for gadolinium based contrasting agents? Water Res. 135, 104–111. https://doi.org/10.1016/j.watres.2017.12.074.

Brünjes, R., Bichler, A., Hoehn, P., Lange, F.T., Brauch, H.-J., Hofmann, T., 2016. Anthropogenic gadolinium as a transient tracer for investigating river bank filtration. Sci. Total Environ. 571, 1432–1440. https://doi.org/10.1016/j.scitotenv.2016.06.105.

Castro, L., Farkas, J., Jenssen, B.M., Piarulli, S., Ciesielski, T.M., 2023. Biomonitoring of rare earth elements in southern Norway: distribution, fractionation, and accumulation patterns in the marine bivalves Mytilus spp. and Tapes spp. Environ. Pollut. 335, 122300.

Crocket, K.C., Hill, E., Abell, R.E., Johnson, C., Gary, S.F., Brand, T., Hathorne, E.C., 2018. Rare earth element distribution in the NE Atlantic: evidence for benthic sources, longevity of the seawater signal, and biogeochemical cycling. Frontiers in Marine Science 5, 147.

Darrah, T.H., Prutsman-Pfeiffer, J.J., Poreda, R.J., Ellen Campbell, M., Hauschka, P.V., Hannigan, R.E., 2009. Incorporation of excess gadolinium into human bone from medical contrast media. Metallomics 1, 479–488.

De Baar, H.J.W., Bacon, M.P., Brewer, P.G., Bruland, K.W., 1985. Rare earth elements in the Pacific and Atlantic oceans. Geochim. Cosmochim. Acta 49, 1943–1959. https://doi.org/10.1016/0016-7037(85)90089-4.

Dulski, P., 1994. Interferences of oxide, hydroxide and chloride analyte species in the determination of rare earth elements in geological samples by inductively coupled plasma-mass spectrometry. Fresenius J. Anal. Chem. 350, 194–203.

Ebeling, A., Zimmermann, T., Klein, O., Irrgeher, J., Pröfrock, D., 2022. Analysis of seventeen certified water reference materials for trace and technology-critical elements. Geostand. Geoanal. Res. 46, 351–378. https://doi.org/10.1111/ggr.12422.

Elderfield, H., Upstill-Goddard, R., Sholkovitz, E.R., 1990. The rare earth elements in rivers, estuaries, and coastal seas and their significance to the composition of ocean waters. Geochim. Cosmochim. Acta 54, 971–991. https://doi.org/10.1016/0016-7037(90)90432-K.

European Medicines Agency, 2017. EMA's Final Opinion Confirms Restrictions on Use of Linear Gadolinium Agents in Body Scans (Opinion No. EMA/625317/2017). European Medicines Agency.

Hale, S.E., Arp, H.P.H., Schliebner, I., Neumann, M., 2020. Persistent, mobile and toxic (PMT) and very persistent and very mobile (vPvM) substances pose an equivalent level of concern to persistent, bioaccumulative and toxic (PBT) and very persistent and very bioaccumulative (vPvB) substances under REACH. Environ. Sci. Eur. 32, 155. https://doi.org/10.1186/s12302-020-00440-4.

Hanana, H., Turcotte, P., André, C., Gagnon, C., Gagné, F., 2017. Comparative study of the effects of gadolinium chloride and gadolinium – based magnetic resonance imaging contrast agent on freshwater mussel, Dreissena polymorpha. Chemosphere 181, 197–207. https://doi.org/10.1016/j.chemosphere.2017.04.073.

Hatje, V., Bruland, K.W., Flegal, A.R., 2016. Increases in anthropogenic gadolinium anomalies and rare earth element concentrations in San Francisco Bay over a 20 year record. Environ. Sci. Technol. 50, 4159–4168.

Henriques, B., Coppola, F., Monteiro, R., Pinto, J., Viana, T., Pretti, C., Soares, A., Freitas, R., Pereira, E., 2019. Toxicological assessment of anthropogenic gadolinium in seawater: biochemical effects in mussels Mytilus galloprovincialis. Sci. Total Environ. 664, 626–634. https://doi.org/10.1016/j.scitotenv.2019.01.341.

Horstmann, M., de Vega, R.G., Bishop, D.P., Karst, U., Doble, P.A., Clases, D., 2021. Determination of gadolinium MRI contrast agents in fresh and oceanic waters of Australia employing micro-solid phase extraction, HILIC-ICP-MS and bandpass mass filtering. J. Anal. At. Spectrom. 36, 767–775.

Idée, J.-M., Port, M., Medina, C., Lancelot, E., Fayoux, E., Ballet, S., Corot, C., 2008. Possible involvement of gadolinium chelates in the pathophysiology of nephrogenic systemic fibrosis: a critical review. Toxicology 248, 77–88. https://doi.org/10.1016/j.tox.2008.03.012.

Kanda, T., Nakai, Y., Oba, H., Toyoda, K., Kitajima, K., Furui, S., 2016a. Gadolinium deposition in the brain. Magnetic Resonance Imaging, Gadolinium Bioeffects and Toxicity 34, 1346–1350. https://doi.org/10.1016/j.mri.2016.08.024.

Kanda, T., Oba, H., Toyoda, K., Kitajima, K., Furui, S., 2016b. Brain gadolinium deposition after administration of gadolinium-based contrast agents. Jpn. J. Radiol. 34, 3–9. https://doi.org/10.1007/s11604-015-0503-5.

Klaver, G., Verheul, M., Bakker, I., Petelet-Giraud, E., Négrel, P., 2014. Anthropogenic rare earth element in rivers: gadolinium and lanthanum. Partitioning between the dissolved and particulate phases in the Rhine River and spatial propagation through the Rhine-Meuse Delta (the Netherlands). Appl. Geochem. 47, 186–197. https://doi.org/10.1016/j.apgeochem.2014.05.020.

Koschinsky, A., Schmidt, K., Paul, S.A.L., Kraemer, D., Ullrich, M., 2020. Tracing origin and distribution of geogenic and anthropogenic dissolved and particulate critical high-technology metals in the southern North Sea, Cruise No. M169, 11.12.2020–29.12.2020, Emden (Germany) - Emden (Germany). DFG Cruise Report. https://doi.org/10.48433/cr_m169.

Kreitsmann, T., Bau, M., 2023. Rare earth elements in alkaline Lake Neusiedl, Austria, and the use of gadolinium microcontamination as water source tracer. Appl. Geochem. 159, 105792 https://doi.org/10.1016/j.apgeochem.2023.105792.

Krohn, Lea M., Klimpel, F., Béziat, P., Bau, M., 2024. Impacts of COVID-19 and climate change on wastewater-derived substances in urban drinking water: evidence from gadolinium-based contrast agents in tap water from Berlin, Germany. Water Res. 121847 https://doi.org/10.1016/j.watres.2024.121847.

Kulaksız, S., Bau, M., 2007. Contrasting behaviour of anthropogenic gadolinium and natural rare earth elements in estuaries and the gadolinium input into the North Sea. Earth Planet. Sci. Lett. 260, 361–371. https://doi.org/10.1016/j.epsl.2007.06.016.

Kulaksız, S., Bau, M., 2011. Anthropogenic gadolinium as a microcontaminant in tap water used as drinking water in urban areas and megacities. Appl. Geochem. 26, 1877–1885. https://doi.org/10.1016/j.apgeochem.2011.06.011.

Kulaksız, S., Bau, M., 2011. Rare earth elements in the Rhine River, Germany: first case of anthropogenic lanthanum as a dissolved microcontaminant in the hydrosphere. Environ. Int. 37 (5), 973–979.

Kulaksız, S., Bau, M., 2013. Anthropogenic dissolved and colloid/nanoparticle-bound samarium, lanthanum and gadolinium in the Rhine River and the impending destruction of the natural rare earth element distribution in rivers. Earth Planet. Sci. Lett. 362, 43–50. https://doi.org/10.1016/j.epsl.2012.11.033.

Lacan, F., Jeandel, C., 2004. Neodymium isotopic composition and rare earth element concentrations in the deep and intermediate nordic seas: constraints on the Iceland Scotland overflow water signature. Geochem. Geophys. Geosyst. 5 (11).

Laukert, G., Frank, M., Bauch, D., Hathorne, E.C., Rabe, B., von Appen, W.-J., Wegner, C., Zieringer, M., Kassens, H., 2017. Ocean circulation and freshwater pathways in the Arctic Mediterranean based on a combined Nd isotope, REE and oxygen isotope section across Fram Strait. Geochim. Cosmochim. Acta 202, 285–309.

Lawrence, M.G., Keller, J., Poussade, Y., 2010. Removal of magnetic resonance imaging contrast agents through advanced water treatment plants. Water Sci. Technol. 61, 685–692.

Le Goff, S., Barrat, J.-A., Chauvaud, L., Paulet, Y.-M., Gueguen, B., Ben Salem, D., 2019. Compound-specific recording of gadolinium pollution in coastal waters by great scallops. Sci. Rep. 9, 8015. https://doi.org/10.1038/s41598-019-44539-y.

Lerat-Hardy, A., Coynel, A., Dutruch, L., Pereto, C., Bossy, C., Gil-Diaz, T., Capdeville, M.-J., Blanc, G., Schäfer, J., 2019. Rare earth element fluxes over 15 years into a major European estuary (Garonne-Gironde, SW France): hospital effluents as a source of increasing gadolinium anomalies. Sci. Total Environ. 656, 409–420.

Lindner, U., Lingott, J., Richter, S., Jiang, W., Jakubowski, N., Panne, U., 2015. Analysis of gadolinium-based contrast agents in tap water with a new hydrophilic interaction chromatography (ZIC-cHILIC) hyphenated with inductively coupled plasma mass spectrometry. Anal. Bioanal. Chem. 407, 2415–2422.

Lingott, J., Lindner, U., Telgmann, L., Esteban-Fernández, D., Jakubowski, N., Panne, U., 2016. Gadolinium-uptake by aquatic and terrestrial organisms-distribution determined by laser ablation inductively coupled plasma mass spectrometry. Environ Sci Process Impacts 18, 200–207. https://doi.org/10.1039/C5EM00533G.

Louis, P., Vignati, D.A.L., Pontvianne, S., Pons, M.-N., 2023. Spatial distribution of rare earth elements in a transnational watershed: the case of the Danube River. Sci. Total Environ. 892, 164368 https://doi.org/10.1016/j.scitotenv.2023.164368.

Macke, M., Quarles Jr., C.D., Sperling, M., Karst, U., 2021. Fast and automated monitoring of gadolinium-based contrast agents in surface waters. Water Res. 207, 117836.

Merschel, G., Bau, M., 2015. Rare earth elements in the aragonitic shell of freshwater mussel Corbicula fluminea and the bioavailability of anthropogenic lanthanum, samarium and gadolinium in river water. Sci. Total Environ. 533, 91–101.

Merschel, G., Bau, M., Baldewein, L., Dantas, E.L., Walde, D., Bühn, B., 2015. Tracing and tracking wastewater-derived substances in freshwater lakes and reservoirs: anthropogenic gadolinium and geogenic REEs in Lake Paranoá, Brasilia. Comptes Rendus-Geoscience 347, 284–293. https://doi.org/10.1016/j.crte.2015.01.004.

Merschel, G., Bau, M., Dantas, E.L., 2017. Contrasting impact of organic and inorganic nanoparticles and colloids on the behavior of particle-reactive elements in tropical estuaries: an experimental study. Geochim. Cosmochim. Acta 197, 1–13. https://doi.org/10.1016/j.gca.2016.09.041.

Möller, P., Dulski, P., 2010. Transmetallation of Gd-DTPA by cu, Y and lanthanides and its impact on the hydrosphere. Appl. Geochem. 25, 48–59. https://doi.org/10.1016/j.apgeochem.2009.09.027.

Möller, P., Dulski, P., Bau, M., Knappe, A., Pekdeger, A., Sommer-Von Jarmersted, C., 2000. Anthropogenic gadolinium as a conservative tracer in hydrology. J. Geochem. Explor. 69–70, 409–414. https://doi.org/10.1016/S0375-6742(00)00083-2.

Möller, P., Knappe, A., Dulski, P., Pekdeger, A., 2011. Behavior of Gd-DTPA in simulated bank filtration. Appl. Geochem. 26, 140–149. https://doi.org/10.1016/j.apgeochem.2010.11.011.

Morteani, G., Möller, P., Fuganti, A., Paces, T., 2006. Input and fate of anthropogenic estrogens and gadolinium in surface water and_ sewage plants in the hydrological basin of Prague (Czech Republic). Environ. Geochem. Health 28, 257–264.

OSPAR Commission, 2000. Quality Status Report 2000: Region II Greater North Sea. OSPAR Commission.

Paffrath, R., Pahnke, K., Behrens, M.K., Reckhardt, A., Ehlert, C., Schnetger, B., Brumsack, H.-J., 2020. Rare earth element behavior in a Sandy subterranean estuary of the southern North Sea. Front. Mar. Sci. 7.

Pereto, C., Lerat-Hardy, A., Baudrimont, M., Coynel, A., 2023. European fluxes of medical gadolinium to the ocean: A model based on healthcare databases. Environ. Int. 173, 107868.

Perrat, E., Parant, M., Py, J.-S., Rosin, C., Cossu-Leguille, C., 2017. Bioaccumulation of gadolinium in freshwater bivalves. Environ. Sci. Pollut. Res. 24, 12405–12415. https://doi.org/10.1007/s11356-017-8869-9.

Pokrovsky, O.S., Schott, J., 2002. Iron colloids/organic matter associated transport of major and trace elements in small boreal rivers and their estuaries (NW Russia). Chem. Geol. Geochem. Crustal Fluids 190, 141–179. https://doi.org/10.1016/S0009-2541(02)00115-8.

Raju, C.S.K., Cossmer, A., Scharf, H., Panne, U., Lück, D., 2010. Speciation of gadolinium based MRI contrast agents in environmental water samples using hydrophilic interaction chromatography hyphenated with inductively coupled plasma mass spectrometry. J. Anal. At. Spectrom. 25, 55–61.

Schijf, J., Christy, I.J., 2018. Effect of mg and ca on the stability of the MRI contrast agent Gd–DTPA in seawater. Front. Mar. Sci. 5.

Schmidt, K., Bau, M., Merschel, G., Tepe, N., 2019. Anthropogenic gadolinium in tap water and in tap water-based beverages from fast-food franchises in six major cities in Germany. Sci. Total Environ. 687, 1401–1408. https://doi.org/10.1016/j.scitotenv.2019.07.075.

Schmidt, K., Paul, S.A.L., Achterberg, E.P., 2022. Assessing the availability of trace metals including rare earth elements in deep ocean waters of the clarion Clipperton zone, NE Pacific: application of an in situ DGT passive sampling method. TrAC Trends Anal. Chem. 155, 116657 https://doi.org/10.1016/j.trac.2022.116657.

Sholkovitz, E.R., 1993. The geochemistry of rare earth elements in the Amazon River estuary. Geochim. Cosmochim. Acta 57, 2181–2190. https://doi.org/10.1016/0016-7037(93)90559-F.

Souza, L.A., Pedreira, R.M.A., Miró, M., Hatje, V., 2021. Evidence of high bioaccessibility of gadolinium-contrast agents in natural waters after human oral uptake. Sci. Total Environ. 793, 148506 https://doi.org/10.1016/j.scitotenv.2021.148506.

Telgmann, L., Faber, H., Jahn, S., Melles, D., Simon, H., Sperling, M., Karst, U., 2012a. Identification and quantification of potential metabolites of Gd-based contrast agents by electrochemistry/separations/mass spectrometry. J. Chromatogr. A 1240, 147–155.

Telgmann, L., Wehe, C.A., Birka, M., Künnemeyer, J., Nowak, S., Sperling, M., Karst, U., 2012b. Speciation and isotope dilution analysis of gadolinium-based contrast agents in wastewater. Environ. Sci. Technol. 46, 11929–11936. https://doi.org/10.1021/es301981z.

Tepe, N., Bau, M., 2016. Behavior of rare earth elements and yttrium during simulation of arctic estuarine mixing between glacial-fed river waters and seawater and the impact of inorganic (nano-)particles. Chem. Geol. 438, 134–145. https://doi.org/10.1016/j.chemgeo.2016.06.001.

Tepe, N., Romero, M., Bau, M., 2014. High-technology metals as emerging contaminants: strong increase of anthropogenic gadolinium levels in tap water of Berlin, Germany, from 2009 to 2012. Appl. Geochem. 45, 191–197. https://doi.org/10.1016/j.apgeochem.2014.04.006.

Turrell, W., 1992. New hyphotheses concerning the circulation of the northern North Sea and its relation to North Sea fish stock recruitment. ICES J. Mar. Sci. 49, 107–123.

Turyanskaya, A., Rauwolf, M., Pichler, V., Simon, R., Burghammer, M., Fox, O.J., Sawhney, K., Hofstaetter, J.G., Roschger, A., Roschger, P., et al., 2020. Detection and imaging of gadolinium accumulation in human bone tissue by micro-and submicro-XRF. Sci. Rep. 10, 6301.

Van De Flierdt, T., Pahnke, K., Amakawa, H., Andersson, P., Basak, C., Coles, B., Colin, C., Crocket, K., Frank, M., Frank, N., et al., 2012. GEOTRACES intercalibration of neodymium isotopes and rare earth element concentrations in seawater and suspended particles. Part 1: reproducibility of results for the international intercomparison. Limnol. Oceanogr. Methods 10, 234–251.

Vassallo, D.V., Simões, M.R., Furieri, L.B., Fioresi, M., Fiorim, J., Almeida, E.A.S., Angeli, J.K., Wiggers, G.A., Peçanha, F., Salaices, M., 2011. Toxic effects of mercury, lead and gadolinium on vascular reactivity. Braz. J. Med. Biol. Res. 44, 939–946.

Wysocka, I.A., Rogowska, A.M., Kostrz-Sikora, P., 2023. Investigation of anthropogenic gadolinium in tap water of polish cities: Gdańsk, Kraków, Warszawa, and Wrocław. Environ. Pollut. 323, 121289 https://doi.org/10.1016/j.envpol.2023.121289.

Xu, A., Hathorne, E., Laukert, G., Frank, M., 2023. Overlooked riverine contributions of dissolved neodymium and hafnium to the Amazon estuary and oceans. Nat. Commun. 14, 4156.

Yeghicheyan, D., Aubert, D., Bouhnik-Le Coz, M., Chmeleff, J., Delpoux, S., Djouraev, I., Granier, G., Lacan, F., Piro, J.-L., Rousseau, T., Cloquet, C., Marquet, A., Menniti, C., Pradoux, C., Freydier, R., Vieira da Silva-Filho, E., Suchorski, K., 2019. A new Interlaboratory characterisation of silicon, rare earth elements and twenty-two other trace element concentrations in the natural river water certified reference material SLRS-6 (NRC-CNRC). Geostand. Geoanal. Res. 43, 475–496. https://doi.org/10.1111/ggr.12268.

Zhang, K., Zocher, A.-L., Bau, M., 2024. Rare earth elements and yttrium in shells of invasive mussel species from temperate rivers in Central Europe: comparison between *C. fluminea*, *D. bugensis*, and *D. polymorpha*. Chem. Geol., 121878 https://doi.org/10.1016/j.chemgeo.2023.121878.

Zocher, A.-L., Klimpel, F., Kraemer, D., Bau, M., 2022. Naturally grown duckweeds as quasi-hyperaccumulators of rare earth elements and yttrium in aquatic systems and the biounavailability of gadolinium-based MRI contrast agents. Sci. Total Environ. 155909.

Zocher, A.-L., Ciesielski, T.M., Piarulli, S., Farkas, J., Bau, M., 2024. Rare earth elements and yttrium (REY) in fjord waters: comparison between seawater in the Trondheimfjord (Norway), its local riverine REY sources and the North Atlantic. Geochim. Cosmochim. Acta. 379, 193–207. https://doi.org/10.1016/j.gca.2024.06.014.